Hindawi
Journal of Food Biochemistry
Volume 2023, Article ID 5824152, 16 pages
https://doi.org/10.1155/2023/5824152

Research Article

The Effect of *Lycium ruthenicum* Murry Anthocyanins on the Apoptosis and Proliferation of H9c2 Cell Induced by Hypoxia

Jinming Li, Mengjie Wang, Hua Wu, Xinlei Chen, Qianwen Xing, Tong Shen, Shuo Wang, and Xiaoqing Wu

College of Agriculture and Animal Husbandry, Qinghai University, Xining, Qinghai 810016, China

Correspondence should be addressed to Hua Wu; qhwuhua@qhu.edu.cn

Received 13 December 2022; Revised 14 June 2023; Accepted 31 July 2023; Published 6 September 2023

Academic Editor: Manoj Oak

Based on the strong antioxidant activity of anthocyanins, this study was aimed to explore the potential influence of *Lycium ruthenicum* Murry anthocyanins (LRMA) on hypoxia-induced apoptosis and proliferation of H9c2 rat cardiomyocytes. The cell viability was first tested after exposure to normoxia, hypoxia, and hypoxia + LRMA. After being incubated for 12 h under normoxia and 24 h under hypoxia in 50 μg/mL LRMA or 100 μM Salidroside, respectively, LDH content, cell morphology, and cell cycle progression were analyzed. In addition, cellular apoptosis along with the expression of B-cell lymphoma-2 (Bcl2) and BCL2-associated X (Bax) was explored. After that, RNA-seq and bioinformatics analysis revealed the lncRNAs-miRNAs-mRNAs ceRNA network related to hypoxia adaptation of H9c2 cells modulated by LRMA. The final step was to detect the expression of cyclin T2 (CCNT2), cyclin-dependent kinase 9 (CDK9), and forkhead box P1 (FOXP1). The results revealed that LRMA significantly attenuated the reduction of viability and protected H9c2 cells under hypoxic condition. In addition, LRMA not only restored the proliferation activity of H9c2 cells but also promoted apoptosis through stimulating Bcl2 enhancement and Bax inhibition induced by hypoxic stimulation. This study also identified distinct pairs of ceRNA and the hypoxia-related differentially expressed genes regulated by LRMA, including 862 lncRNAs (694 upregulated and 168 downregulated), 7 miRNAs (1 upregulated and 6 downregulated), and 351 mRNAs (226 upregulated and 125 downregulated). The results also suggested that the hypoxia-related genes regulated by LRMA were mainly enriched in cell proliferation and division, cell energy metabolism, inflammatory response, and cell development. However, LRMA could effectively promote the proliferation of H9c2 cells through enhancing CCNT2, CDK9, and FOXP1 under hypoxic conditions. Overall, LRMA could alleviate the proliferation inhibition and apoptosis in hypoxia-induced H9c2 cells.

1. Introduction

In 1947, Jack, who was studying at Bordeaux University in France, first discovered a novel substance from the peanut skin and named it anthocyanin [1]. It is a water-soluble flavonoid, which primarily exists in different forms in the cell fluid of a variety of plants, such as the fruits of *Lycium ruthenicum* Murry, seabuckthorn, black mulberry, blueberry, purple potato, and cherry [2]. It has been reported that anthocyanins can be found in different colors such as red, blue, and purple and can exist in acidic, alkaline, and neutral environments, respectively. The six most common anthocyanidins identified are pelargonidin, cyanidin, delphinium, peonidin, petunidin, and malvidin chloride [3]. More importantly, it has been found to be valuable in medical research for its characteristics of strong antioxidant, anti-inflammatory, and antitumor activities [4–6] and its reported role in the prevention of the cardiovascular disease.

Lycium ruthenicum Murry is an undeveloped wild resource of medlar plant in the northwest of China, whose fruit is spherical, nontoxic, and sweet with purple black color, being famous as "Desert Black Pearl" and "King of anthocyanidin" for its rich anthocyanidins. It has been reported that the risk of cardiovascular disease can be effectively reduced by regular intake of the fruits and foods rich in anthocyanin [7]. In addition, negative correlation has been

also reported between anthocyanin intake and the risk of myocardial infarction as well as cardiovascular disease-related mortality from epidemiological data [8], indicating that anthocyanin might play an important preventive role in cardiovascular disease.

The heart is extremely sensitive to oxygen, so a high correlation has been reported between the occurrence and development of heart diseases and hypoxia [9]. Ischemia and hypoxia can effectively lead to cardiomyocyte injury and cardiac dysfunction, which have been assigned as the main reason of ischemic heart disease and sudden death [10]. Therefore, it is of great value to detect novel strategies to improve the hypoxic adaptability of cardiomyocytes. Furthermore, Wang et al. [11] found that cardiomyocyte injury induced by hypoxia could be markedly relieved through improving glucose metabolic rate by modulating lncRNA-XIST-miR-125b-Hexokinase2. In addition, Wang et al. [12] indicated that hypoxic injury of cardiomyocytes can be aggravated through autophagy mediated by lncRNA-MALAT1-miR-20b-Beclin1 axis. A number of prior reports have also demonstrated that hypoxia-induced cardiomyocyte injury can be regulated by lncRNAs-miRNAs-mRNAs ceRNA network. Herein, we have analyzed the potential effects of LRMA on hypoxic adaptation and constructed a network of lncRNAs-miRNAs-mRNAs to explore the mechanism of gene exchange and hypoxic protection regulated by LRMA in H9c2 cells. The study aimed to lay a solid groundwork for the research on the adaptability of mammals in hypoxic environment and to provide a theoretical basis for application of LRMA in improving the hypoxic adaptation of mammals in the plateau.

2. Materials and Methods

2.1. Reagents. Dulbecco's modified Eagle's medium (DMEM), penicillin and streptomycin, pancreatic, and fetal bovine serum (FBS) were purchased from Gibco (Beijing, China). Phosphate buffered saline (PBS) and Salidroside (Sal) were purchased from Solarbio in China. LRMA was purchased from Qinghai Jinmaiqi Biotechnology Co., Ltd in China. Cell Counting Kit-8 (CCK-8) kit, lactate dehydrogenase (LDH) cytotoxicity assay kit, reactive oxygen species (ROS) assay kit, cell cycle and apoptosis analysis kit, Bax, Bcl2, CDK9 rabbit polyclonal antibody, and HRP-labeled goat anti-rabbit IgG (H + L) were procured from Beyotime. CCNT2 and FOXP1 were obtained from Proteintech. PCR primers were obtained from Sangon Biotech. The rat cardiomyocytes H9c2 were purchased from ATCC (Manassas, VA, USA).

2.2. Reagent Preparation. Preparation of LRMA solution: accurately weigh 0.01 g of LRMA and dissolve it in 10 mL of DMEM medium. Prepare 1 mg/mL of LRMA master mix and store at −20°C.

2.3. Cell Culture. H9c2 cells were cultured in DMEM at 37°C in the presence of 95% air and 5% CO_2. Besides, H9c2 cells were cultured in DMEM at 37°C using hypoxic chambers with 1% O_2, 94% N_2, and 5% CO_2 for 24 h to build hypoxic model. According to the previous findings of our research group, the optimal concentration of LRMA was 50 μg/ml. Therefore, subsequent experiments were carried out at this specific concentration. H9c2 cells were counted in cell counting plates for application in different assays and then collected or analyzed accordingly.

2.4. Cell Viability Assay. H9c2 cells were seeded in 96-well plates at 1×10^5 cells/well and cultured at 37°C with 95% air and 5% CO_2 for 24 h. The cells were induced by LRMA (0, 12.5, 25, 50, and 100 μg/mL) for 0, 12, 24, 36, and 48 h in normoxic or hypoxic condition, respectively. Thereafter, cell viability was analyzed by CCK-8 kit.

2.5. LDH Activity Assay. H9c2 cells were planted in 96-well plates at 1×10^5 cells/well and cultured at 37°C with 95% air and 5% CO_2 for 24 h. Thereafter, 50 μg/mL LRMA was added for 12 h under normoxia + 24 h under hypoxic condition, and LDH activity was measured by using the LDH kit.

2.6. Cell Cycle Analysis. H9c2 cells were seeded in 6-well plates at 1×10^6 cells/well. This was followed by 50 μg/mL LRMA or 100 μM Sal treatment for 12 h under normoxia + 24 h under hypoxic condition, respectively. The cells were then digested with trypsin and were fixed overnight in a 4°C refrigerator with 70% ethanol. After that, the cells were washed twice with PBS, resuspended by 500 μL staining solution (PI : RNase = 1 : 9), and incubated in dark for 30 min. Finally, cell cycle progression was detected by flow cytometry (BECKMAN COULTER, Xining, Qinghai, China).

2.7. Hoechst33342/PI Stain. H9c2 cells were seeded in 6-well plates at 1×10^6 cells/well and cultured as described in 2.5. The cells were then washed with PBS two times and stained with Hoechst 33342 and Propidium Iodide (PI). Thereafter, the fluorescence of cells was detected by an inverted fluorescence microscope (Olympus IX83, Xining, Qinghai, China).

2.8. Analysis of ROS Accumulation. H9c2 cells were seeded in 6-well plates at 1×10^6 cells/well and cultured as described above in 2.6. Thereafter, DCFH-DA was diluted 1000 times in the serum free medium and 10 μL of Rosup was added to the positive control group, followed by incubation for 30 min. After loading DCFH-DA fluorescent probe in situ, the cells were then washed twice to completely remove the unloaded probe and the fluorescence intensity was measured by fluorescent microplate reader

(Bio-Rad, Xining, Qinghai, China). The excitation wavelength was 502 nm and the emission wavelength was 530 nm.

2.9. Measurement of Apoptosis. H9c2 cells were seeded in 6-well plates at 1×10^6 cells/well and cultured as described above in 2.6. The cells and supernatants were collected and resuspended in 500 μL buffer and stained with 5 μL annexin V and 5 μL PI for 10 min. The apoptosis rate was detected by flow cytometry (BECKMAN COULTER, Xining, Qinghai, China).

2.10. RNA-Seq Analysis. H9c2 cells were seeded in 6-well plates at 1×10^5 cells/well and cultured as described above in 2.5. The total RNA was isolated from H9c2 cells by using Trizol reagent, and RNA-seq was performed.

2.10.1. Analysis of the Differentially Expressed Genes. The differentially expressed genes were compared between Hyp group and Hyp + LRMA group and Nor group and Hyp group. Then, they were processed and analyzed by the edgeR package in *R* language version 4.0.2. The significant differences in lncRNA, mRNA, and miRNA data were detected by logFC ≥ 1 and FDR < 0.05.

2.10.2. Metascape Pathway Enrichment Analysis. The pathway enrichment analysis of mRNA was performed by Metascape (online tools: https://metascape.org/gp/index.html). The graphs in *R* language version 4.2.0 were created by ggplot2 package. The significant difference in the results was tested by FDR < 0.05.

2.10.3. Interactions between miRNAs and mRNAs and between IncRNAs and miRNAs. According to the expression of lncRNA, miRNA, and mRNA from RNA-seq, the possible correlation between lncRNAs and miRNAs and miRNAs and mRNAs was assessed by Pearson correlation analysis. After identification, it was correlated with both $r > 0.8$ and $P < 0.05$. Thereafter, correlations in both miRNAs-mRNAs and miRNAs-lncRNAs were predicted by TargetScan.

2.10.4. Construction of the Competing Endogenous RNA (ceRNA) Network. The competing endogenous RNA (ceRNA) network was constructed from the data obtained about the differential expression of miRNAs, mRNAs, and lncRNAs. The cross-linking relationship and network construction was performed by using Cytoscape version 3.8.2.

2.11. qRT-PCR. Total RNA was isolated from H9c2 cells by using Trizol reagent and then reversed transcription to cDNA in accordance with the manufacturer's instructions (Table 1). The expression of miRNA was detected by tailing reaction. The representative gene expression data were normalized with β-actin expression by using the following formula: $2^{-\triangle\triangle ct}$. The various constituents used for qRT-PCR are shown in Table 2.

Table 1: Reagents used for reverse transcription.

Reagent	Volume
5 × FastKing-RT super mix	4.0 μL
Total RNA	50 ng–2.0 μg
RNase free ddH_2O	Make up to 20 μL

PCR primers were as follows: ENSRNOT00000076766 (Forward: TACCCAAGGGCCTCCTCCAATG; Reverse: TTCCCATATTTGCAGCTCCTTCTGG), ENSRNOT00000093358 (Forward: GCCGAGCCTGCTGACATATAGAAG; Reverse: TGGTTCAGATGAGAGGTGGCAAATC), rno-miR-98-5p (Forward: ACGAGCGCTGAGGTAGTAAGTTGT), rno-miR-29c-3p (Forward: GCGCTAGCACCATTTGAAATCGGT), U6 (Forward: AGAGAAGATTAGCATGGCCCCTG), Bax (Forward: AGACACCTGAGCTGACCTTGGAG; Reverse: TTCATCGCCAATTCGCCTGAGAC), Bcl2 (Forward: CCGTCGTGACTTCGCAGAGATG; Reverse: ATCCCTGAAGAGTTCCTCCACCAC), CCNT2 (Forward: TCCCTGCTCCACTACCTCTAACTTC; Reverse: TGGCTGAGTCTGGATGGTGAGG), CDK9 (Forward: TTAAAGCCAAGCACCGTCAGACC; Reverse: TGATTTCCCGCAAGGCTGTGATG), FOXP1 (Forward: CAGCAACAGCAGCAACAGCAAC; Reverse: CATCATAGCCACTGACACGGGAAC), and GADPH (Forward: TGCTCTGCACCACATATAGTGACT; Reverse: TGCTGGTGTAGTTTGCTGGTGCAA).

2.12. Western-Blot Analysis. H9c2 cells were seeded in 6-well plates at 1×10^6 cells/well. The cells were then exposed to 50 μg/mL LRMA and 100 μM Sal incubation for 12 h under normoxia + 24 h under hypoxic condition, respectively. The whole cell extract was prepared and quantified by using the bicinchoninic acid (BCA) method as described previously [13] (Table 3).

Thereafter, equal amounts of proteins were subjected to sodium dodecyl-sulfate polyacrylamide gel electrophoresis (SDS-PAGE) electrophoresis (Tables 4 and 5).

The proteins were then transferred to polyvinylidene fluoride (PVDF) membrane and then sealed with 5% skimmed milk at room temperature for 1.5 hours. Thereafter, PVDF membrane was washed with PBST for 3 minutes and this process was repeated for 5 times. The membrane was then incubated with the primary antibody diluted at an appropriate concentration for overnight at 4°C. Next day, the membrane was washed with PBST for 10 minutes and this procedure was repeated for 5 times. After washing, diluted secondary antibody was added to the membrane and incubated at 37°C for 1 hour. After washing with PBST again slowly for 30 minutes (3 times), appropriate amount of prepared ECL luminescent solution was added to the PVDF film, and it was incubated in the dark room for 1~2 min. The membrane was scanned and imaged with bio rad gel imager and obtained bands were analyzed with bio rad image analysis software (Quantity One® 1-D Analysis Software), and the corresponding optical density values of the bands were recorded.

Table 2: The various constituents used for qRT-PCR.

Constituent ingredients	20 μL system (μL)
2 × SuperReal color PreMix	10
Forward primers (10 μM)	0.6
Reverse primers (10 μM)	0.6
cDNA template (contain dilution buffer)	2
RNase-free ddH_2O	6.8

Table 3: BSA standard preparation table.

Standard no.	Diluent volume (μl)	Standard product consumption (μl)	Standard concentration (μg/ml)
1	0	20	500
2	4	16	400
3	8	12	300
4	12	8	200
5	16	4	100
6	20	0	0

Table 4: 10% SDS-PAGE separating gel.

Reagent	Volume (ml)
30% acrylamide	3.30
1.5 mol/L tris Hcl (pH 8.8)	2.50
10% SDS	0.01
ddH_2O	4.00
10% ammonium persulfate	0.01
TEMED	0.01
Total volume	10

Table 5: 5% SDS-PAGE concentrated gel.

Reagent	Volume (ml)
30% acrylamide	0.830
1 mol/L tris Hcl (pH 6.8)	0.625
10% SDS	0.050
ddH_2O	3.420
10% ammonium persulfate	0.075
TEMED	0.008
Total volume	5

3. Results

3.1. LRMA Mitigated Proliferation Reduction of H9c2 Cells and Played a Protective Role against Hypoxia. We first studied the protective effect of LRMA on H9c2 cells. The results indicated that the viability of the cells treated with 25 and 50 μg/mL LRMA for 24, 36, and 48 h was significantly upregulated in normoxia ($P < 0.05$; Figure 1(a)). Figure 1(b) displays that compared with the normoxia group after hypoxia treatment, cell activity was significantly reduced ($P < 0.05$). Different concentrations of LRMA induced H9c2 rat cardiomyocytes for 24 h, 36 h, and 48 h significantly increased cell activity compared with the hypoxic group ($P < 0.05$), and the cardiomyocyte activity of H9c2 rats was increased after 12 h of induction, but the difference was not significant ($P > 0.05$). Comparison between concentration groups revealed that 50 μg/mLLRMA had the best effect in protecting cardiomyocyte activity in H9c2 rats, and comparison between time groups revealed that LRMA induced the best protective effect on cardiomyocytes in H9c2 rats for 36 h. This finding suggested that the optimal strategy to protect the viability of H9c2 cells could be treating cells with 50 μg/mL LRMA for 12 h under normoxia + 24 h under hypoxic condition, and thus it was used for the subsequent experiments. The next step was to observe LDH activity and cell morphology to examine whether the hypoxia model was constructed successfully or not. Figure 1(c) displays that hypoxia substantially elevated LDH activity ($P < 0.01$), whereas LRMA noticeably alleviated the LDH accumulation aroused by hypoxia ($P < 0.05$). Moreover, both the cell count and morphology were remarkably relieved by hypoxia but augmented upon LRMA treatment (Figure 1(d)). In addition, salidroside (Sal), one of the main components of Rhodiola, could also alleviate the observed effects of hypoxia. Figure 1(e) shows that LRMA effectively promoted the proliferation of H9c2 cells by alleviating the cell cycle arrest induced by hypoxia ($P < 0.05$). Under hypoxic conditions ($P > 0.05$), there was no significant difference noted between LRMA and Sal on the promotion of proliferation in H9c2 cells. Taken together, LRMA could modulate the proliferation of H9c2 cells and played a protective role in H9c2 cells under hypoxic conditions.

3.2. LRMA Mitigated H9c2 Cell Apoptosis Promoted by Hypoxia. We further explored the potential effect of LRMA on apoptosis in H9c2 cells under hypoxic condition and harvested the cells after the treatment. Interestingly, Figure 2(a) showed that H9c2 cells under hypoxic condition displayed notably brighter fluorescence, whereas LRMA treatment significantly reversed the fluorescence intensity aroused by hypoxia. Further study was performed next, which demonstrated that hypoxia remarkably augmented the ROS content, apoptosis rate, and Bax expression, but declined Bcl2 level and Bcl2/Bax ratio in H9c2 cells ($P < 0.01$). On the contrary in Hyp + LRMA and Hyp + Sal groups, the ROS content, apoptosis rate, and Bax expression were obviously lowered, but Bcl2 expression and Bcl2/Bax ratio were enhanced in Hyp + LRMA and Hyp + Sal groups ($P < 0.01$) (Figures 2(b)–2(e)). However, LRMA and Sal had exhibited no significant effect on cell apoptosis. Consequently, it was concluded that LRMA protected H9c2 cells by inhibiting apoptosis under hypoxic condition.

3.3. Identification of the Hypoxia-Related ceRNA Network Regulated by LRMA. RNA-seq and bioinformatics analysis were performed to construct the hypoxia-related ceRNA network and to explore the target axis of hypoxia injury and the potential molecular mechanisms of hypoxia adaptation in H9c2 cells affected by LRMA.

The results indicated that there were 1404 differentially expressed lncRNAs (525 upregulated and 879 downregulated), 20 miRNAs (12 upregulated and 8 downregulated), and 829 mRNAs (609 upregulated and 220 downregulated). These were controlled primarily by hypoxia

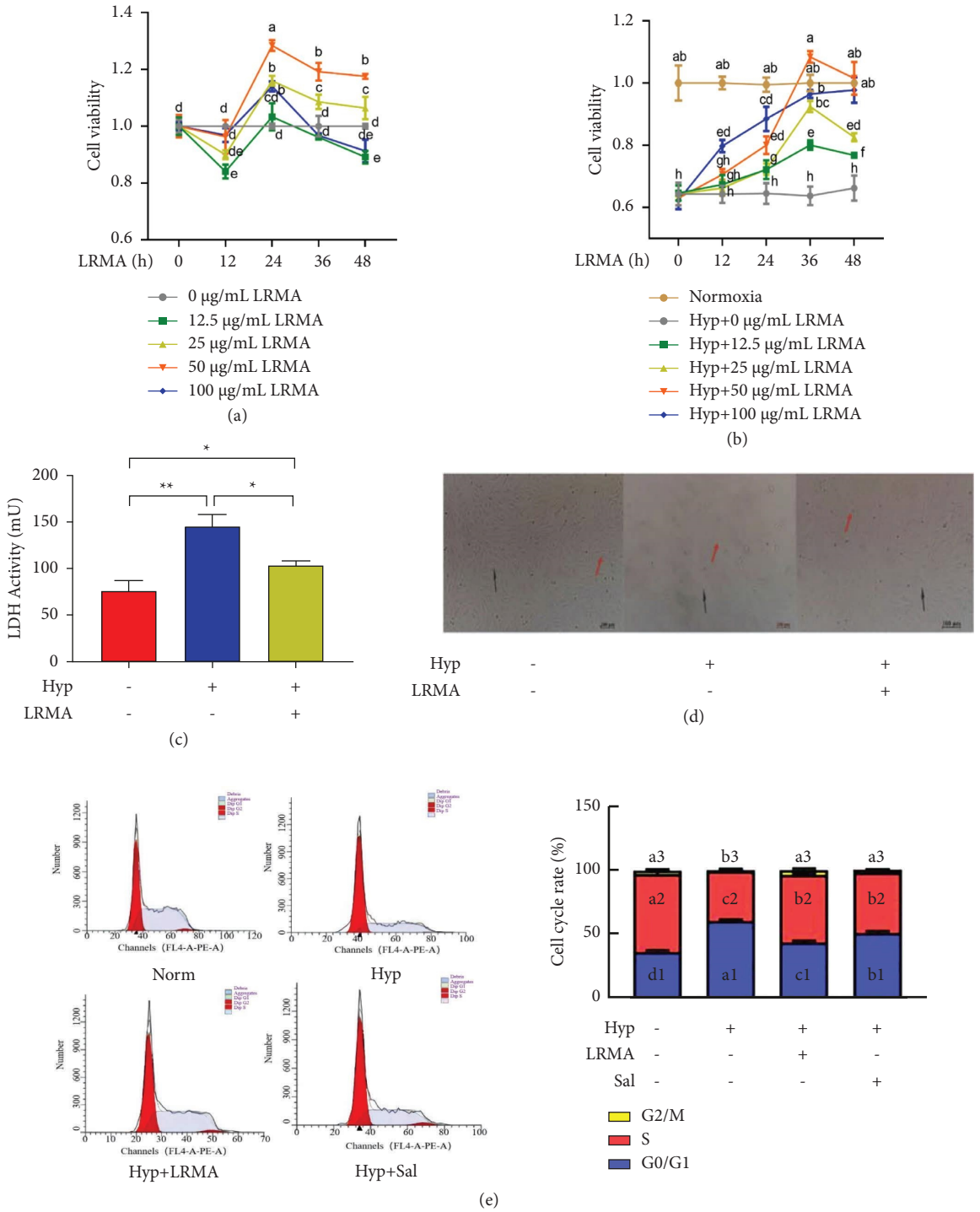

FIGURE 1: LRMA protected H9c2 cell viability reduction in hypoxia. H9c2 cells were exposed to LRMA (0, 12.5, 25, 50, and 100 μg/mL) for 0, 12, 24, 36, and 48 h in normoxia (a) or hypoxia for 24 h (b), respectively. Thereafter, the cell viability was analyzed. Next, followed by 50 μg/mL LRMA incubation for 24 h under hypoxic condition, LDH activity (c), morphological changes (d), and cell cycle distribution (e) of H9c2 cells were tested, respectively. $N = 3$. Different letters mean significant differences ($P < 0.05$) while the same letter indicates no significant difference ($P > 0.05$). $^{*}P < 0.05$ and $^{**}P < 0.01$. NS: no significance.

between Norm group and Hyp group. Moreover, we observed that differentially expressed 1769 lncRNAs (1141 upregulated and 628 downregulated), 63 miRNAs (36 upregulated and 27 downregulated), and 2517 mRNAs (2047 upregulated and 470 downregulated) were controlled by LRMA under hypoxic condition between Hyp group and Hyp + LRMA group. By taking the intersection of these differentially expressed genes, we obtained the hypoxia-related differentially expressed genes regulated by LRMA. These included 862 lncRNAs (694 upregulated and 168

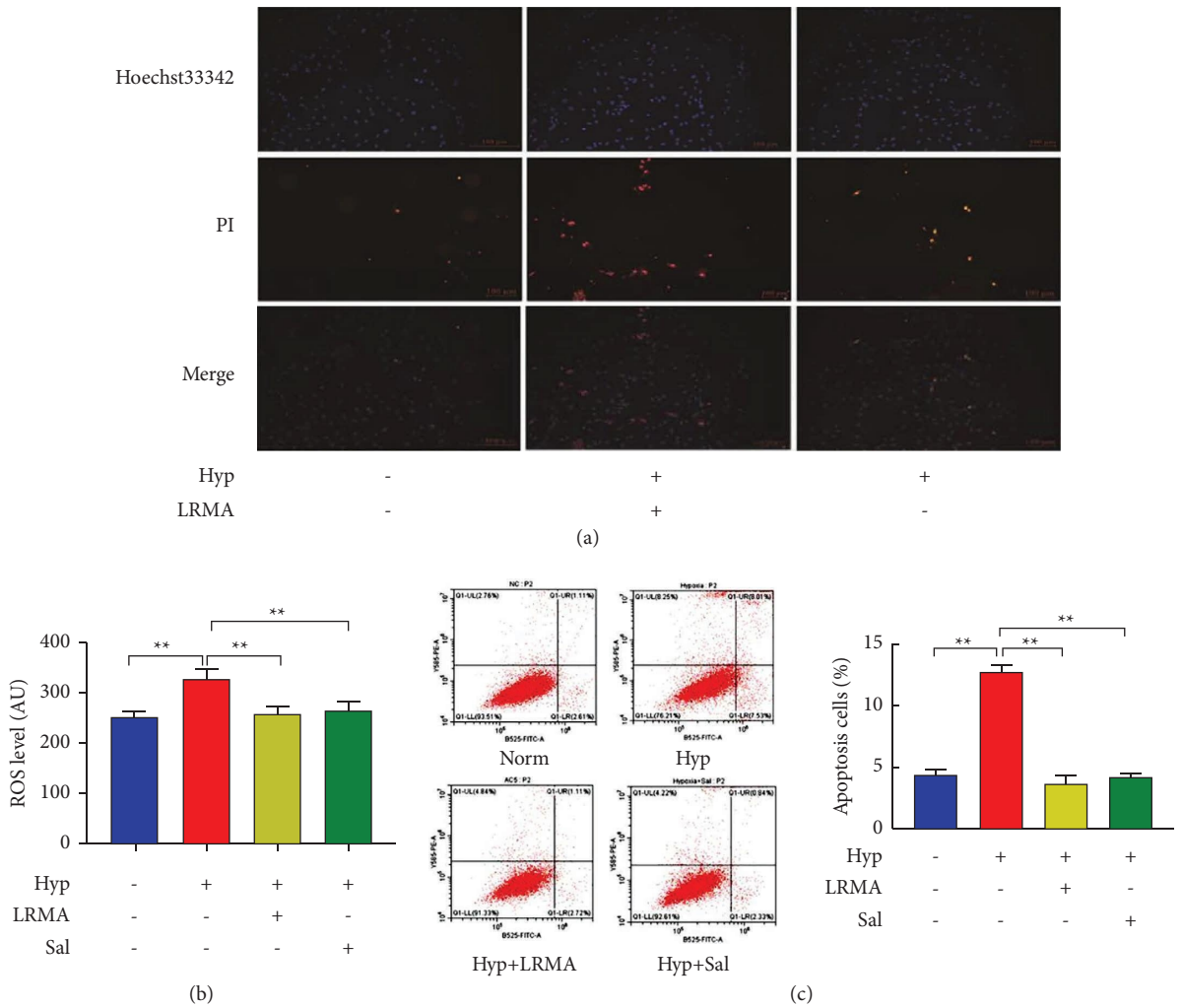

Figure 2: Continued.

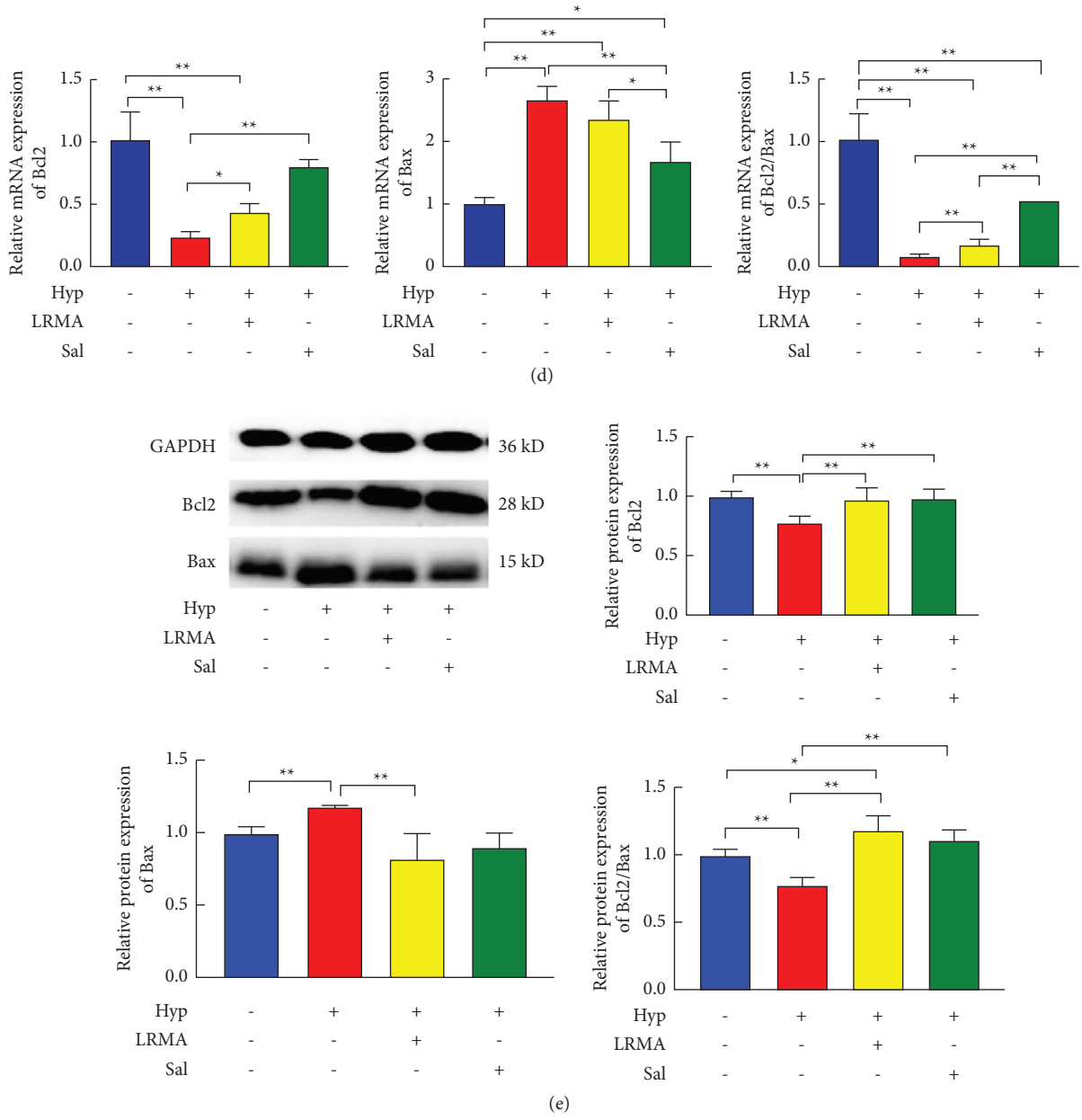

Figure 2: LRMA attenuated H9c2 cell apoptosis caused by hypoxia. After exposure of H9c2 cells to 50 μg/mL LRMA incubation for 12 h under normoxia + 24 h under hypoxic condition, Hoechst33343/PI was performed to analyze apoptotic cells. (a) In addition, 50 μg/mL LRMA and 100 μM sal were incubated for 12 h under normoxia + 24 h under hypoxic condition, respectively, and ROS content (b) as well apoptotic rate (c) of H9c2 cells were examined. Then, the Bcl2, Bax, and Bcl2/Bax expressions at mRNA (d) and protein (e) level were detected, respectively. $N = 3$. $^{*}P < 0.05$ and $^{**}P < 0.01$. NS: no significance.

downregulated), 7 miRNAs (1 upregulated and 6 downregulated), and 351 mRNAs (226 upregulated and 125 downregulated) (hypoxia-related differential expressed lncRNAs, miRNAs, and mRNAs regulated by LRMA have been shown in Tables 1–3 of supplementary materials, respectively). Then, hierarchical cluster analysis was performed to explore the possible phenotypic differences of transcriptome regulated by LRMA under the hypoxic conditions. The differentially expressed lncRNAs, miRNAs, and mRNAs indicated that there were obvious differences in Norm group, Hyp group, and Hyp + LRMA group, but some of them were similar while others were different in Norm group and Hyp + LRMA group (Figures 3(a)–3(c)).

Figure 3 and Table 1 exhibit that there were 12 specific pathway enrichment projects of differentially expressed mRNA, including heatmap and Venn of lncRNA (Figure 3(a)), miRNA (Figure 3(b)), and mRNA (Figure 3(c)) were constructed. In addition, the bubble chart of pathway enriched by metascape (https://metascape.org/gp/index.html) was plotted (Figure 3(d)). Furthermore, ceRNA network was also built by cytoscape_v3.8.2 (Figure 3(e)). $N = 3$. However, hypoxia-related genes

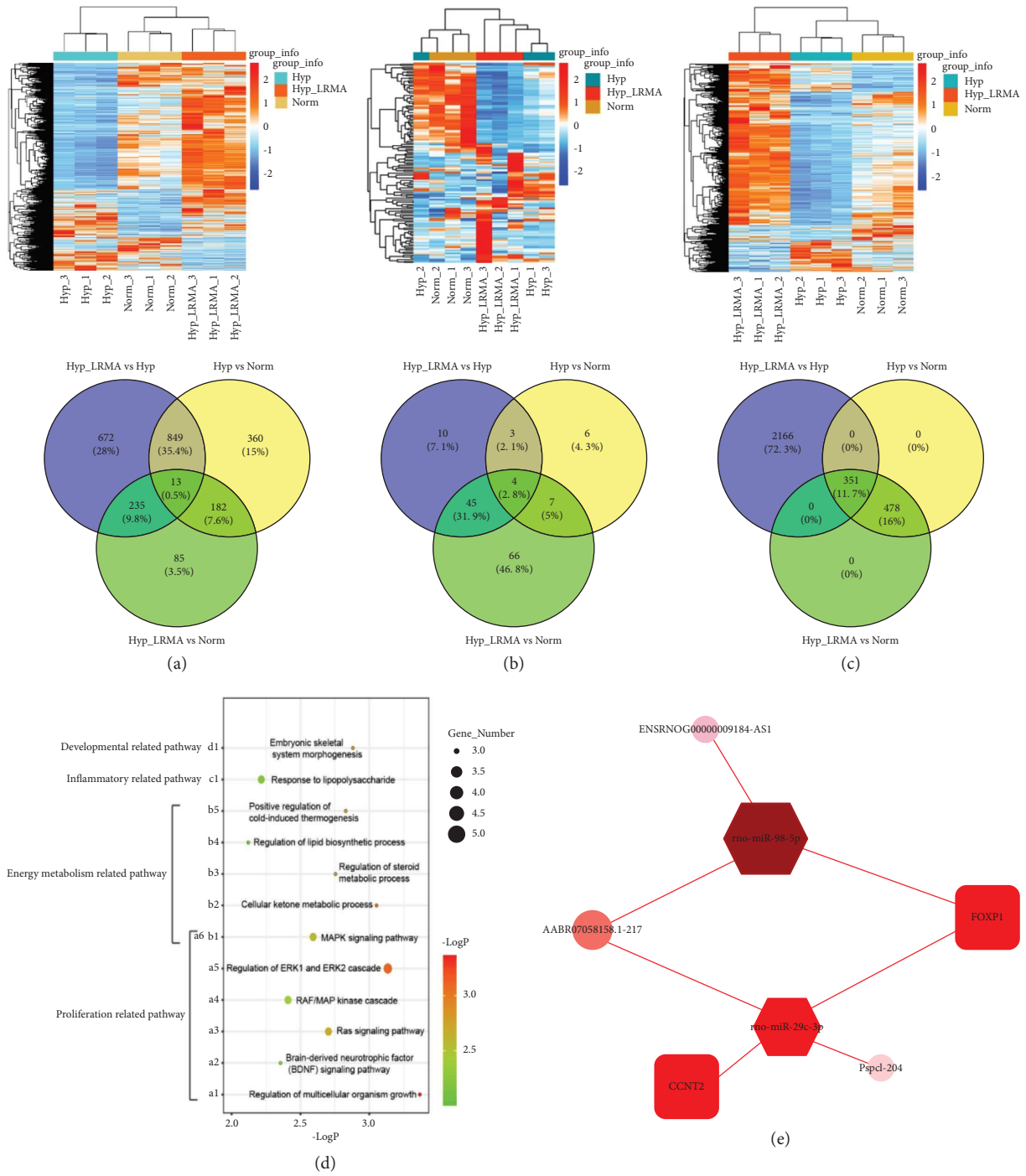

Figure 3: Bioinformatics analysis. H9c2 cells were treated with 50 μg/mL LRMA for 12 h under normoxia + 24 h under hypoxic condition, and thereafter RNA-seq was performed. Then, heatmap and venn of lncRNA (a), miRNA (b), and mRNA (c) were constructed. In addition, the bubble chart of pathway enriched by metascape (https://metascape.org/gp/index.html) was plotted. (d) However, ceRNA network was built by cytoscape_v3.8.2 (e). $N = 3$.

regulated by LRMA were mainly enriched in cell proliferation and division (regulation of multicellular organization growth, brain derived neurotrophic factor (BDNF) signaling pathway, Ras signaling pathway, Raf/MAP kinase cascade, and the regulation of ERK1 and ERK2 cascade and MAPK signaling pathway). They were also enriched in the cell energy metabolism (MAPK signaling pathway, cellular ketone metabolic process, regulation of steroid biosynthetic process, regulation of lipid biosynthetic process, and the positive regulation of cold induced thermogenesis), inflammatory response (response to lipopolysaccharide), and cell development (morphogenesis of embryonic skeletal system) (Table 6). Therefore, we speculated that hypoxia adaptation of H9c2 cells might be regulated by LRMA

Table 6: Metascape functional enrichment pathway of the differential hypoxia-related mRNA regulated by LRMA.

GO/KEGG/Wiki/Reactom ID and item	Category	Gene count	Fold enrichment	Log_{10} (P)
GO: 0040014 and regulation of multicellular organism growth	GO biological processes	3	4.29	−3.35
WP2380 and brain-derived neurotrophic factor (BDNF) signaling pathway	Wiki pathways	8	11.43	−4.90
hsa04014 and ras signaling pathway	KEGG pathway	4	5.71	−2.68
R-HSA-5673001 and RAF/MAP kinase cascade	Reactome gene sets	4	5.71	−2.41
GO: 0070372 and regulation of ERK1 and ERK2 cascade	GO biological processes	5	7.14	−3.13
WP382 and MAPK signaling pathway	Wiki pathways	4	5.71	−2.59
GO: 0042180 and cellular ketone metabolic process	GO biological processes	3	4.29	−3.05
GO: 0019218 and regulation of steroid metabolic process	GO biological processes	3	4.29	−2.75
GO: 0046890 and regulation of lipid biosynthetic process	GO biological processes	3	4.29	−2.12
GO: 0120162 and positive regulation of cold-induced thermogenesis	GO biological processes	3	4.29	−2.81
GO: 0032496 and response to lipopolysaccharide	GO biological processes	4	5.71	−2.22
GO: 0048704 and embryonic skeletal system morphogenesis	GO biological processes	3	4.29	−2.88

through modulation of the cell proliferation and division, cell energy metabolism, inflammatory response, and cell development.

ceRNA can regulate the expression of the various gene transcripts by competing for reaction elements bind to the same miRNA. We did screening parameters: correlation ≥0.6 and P value ≤0.05. Thereafter, lncRNAs-miRNAs-mRNAs regulatory network was constructed by Pearson correlation analysis and targetscan database prediction. Finally, 8 lncRNA-miRNA pairs and 33 miRNA-mRNA pairs were obtained (showed in the list 10 of supplementary materials (available here)), and 5 pairs of lncRNAs-miRNAs-mRNAs (ENSRONG09184-ASL-rno-miR-98-6p-FOXP1, AABR0758158.1-217-rno-miR-98-6p-FOXP1, AABR0758158.1-217-rno-miR-29c-3p-FOXP1, AABR0758158.1-217-rno-miR-29c-3p-CCNT2, and Pspc1-204-rno-miR-29c-3p-CCNT2) were analyzed (Figure 3(e)). The expression of the most significant key nodes in the ceRNAs network was assessed by qRT-PCR (Pspc-1-204, AABR07058158.1-217, miR-98-5p, miR-29c-3p, CCNT2, and FOXP1). The results of qRT-PCR and high-throughput sequencing were found to be completely consistent in the expression patterns (Figures 4(a)–4(c)), thus indicating that key genes in the ceRNAs regulatory network regulated by LRMA were objective and reliable.

CCNT2, a highly conserved member of cyclin family, can regulate the activity of cyclin dependent kinase. It is periodically expressed in the cell cycle and significantly correlated with myocardial ischemia reperfusion, acute myeloid leukemia, cancer, acute nephropathy, and other diseases [13–16]. Furthermore, CCNT2 and CDK9 can substantially promote the translation and form heterodimer by phosphorylating the C-terminal of the large subunit in RNA polymerase II and activating the positive transcription elongation factor b (p-TEFb) to accelerate the cell cycle progression [17]. On the other hand, by combining DNA with its conserved forkhead DNA binding domain, FOXP1, a transcription factor, it can influence the cell proliferation, differentiation, and metabolic pathways, such as embryonic stem cell pluripotency, cardiomyocyte proliferation, neuronal activity, and glucose homeostasis [18]. FOXP1 has been reported to be expressed in the whole heart, including myocardium, endocardium, and endocardial cushion [19]. However, it plays an extremely pivotal role in the regulation of the proliferation, differentiation, and angiogenesis of heart [20]. In this study, we found that LRMA effectively protected the proliferative activity of H9c2 cells aroused by hypoxia, which may be interrelated to these 5 pairs of ceRNAs. In addition, LRMA dramatically enhanced expression of CCNT2 and FOXP1 under hypoxic condition. Therefore, we speculated that LRMA might protect the proliferative activity and hypoxic adaptability of H9c2 cells under hypoxic condition by CCNT2 and FOXP1. Based on the result of RNA-seq, further study was performed by analyzing the expression of both CCNT2 and FOXP1. Figures 4(d) and 4(e) show that hypoxia markedly declined the CCNT2, CDK9, and FOXP1 expression in H9c2 cells ($P < 0.01$). On the contrary, in H9c2 cells stimulated by hypoxia, LRMA substantially increased the CCNT2, CDK9, and FOXP1 expression. In addition, under hypoxic conditions ($P > 0.05$), the regulation of CCNT2, CDK9, and FOXP1 expression in H9c2 cells by LRMA and Sal was not found to be significantly different.

4. Discussion

Cell proliferation is the basis for growth, development, reproduction, and genetics of organisms, and the traditional concept is that cardiomyocytes are terminally differentiated cells that cease to participate in the cell cycle process shortly after birth and no longer have the ability to proliferate [21, 22], but it has been found that cardiomyocyte proliferation after myocardial injury is a necessary process for restoring myocardial function [23], so it is particularly important to protect the proliferative activity of cardiomyocytes induced by hypoxia. Anthocyanins are water-soluble natural pigments with good antioxidant activity, which can effectively alleviate hypoxia-induced cardiomyocyte apoptosis and myocardial damage. However, no study has been reported on the effects of LRMA on hypoxia-induced proliferation and apoptosis in H9c2 rat cardiomyocytes.

In this study, the effect of LRMA on the proliferation viability of H9c2 rat cardiomyocytes under hypoxia was investigated for the first time. It was found that the addition of LRMA significantly increased the activity of H9c2 rat cardiomyocytes induced by 25 and 50 μg/mL LRMA for 24, 36, and 48 h under normoxic conditions and that 100 μg/mL LRMA induced H9c2 rat cardiomyocytes for 24 h was able to significantly increase the activity of H9c2 rat cardiomyocytes. Under hypoxic conditions, different concentrations of LRMA induced in H9c2 rat cardiomyocytes for 12, 24, 36, and 48 h could effectively improve the H9c2 rat cardiomyocyte activity, indicating that LRMA could effectively protect the cell proliferation activity of H9c2 rat cardiomyocytes under hypoxic conditions, among which 50 μg/mL LRMA induced for 36 h had the best protective effect on H9c2 rat cardiomyocyte activity. Based on the above results, the optimal induction protocol for LRMA under hypoxic conditions was screened as follows: 50 μg/mL LRMA pretreatment for 12 h, while the cells were then placed under hypoxic + LRMA conditions and continued to be induced for 24 h.

Sal has various effects such as good antioxidant and free radical scavenging [24] and protective effect on myocardial ischemia [25], so it was used as a positive control group in this experiment to compare and test the effect of LRMA on hypoxia-induced proliferation and apoptosis of H9c2 rat cardiomyocytes. In this experiment, it was found using flow cytometry that LRMA could effectively alleviate the cell cycle arrest of H9c2 rat cardiomyocytes under hypoxic conditions and promote cell cycle progression, thus promoting the proliferation of H9c2 rat cardiomyocytes. Under hypoxic conditions, there was no significant difference between LRMA and Sal in promoting H9c2 cell proliferation. In summary, LRMA can regulate the proliferation of H9c2 cells and protect these cells under hypoxic conditions.

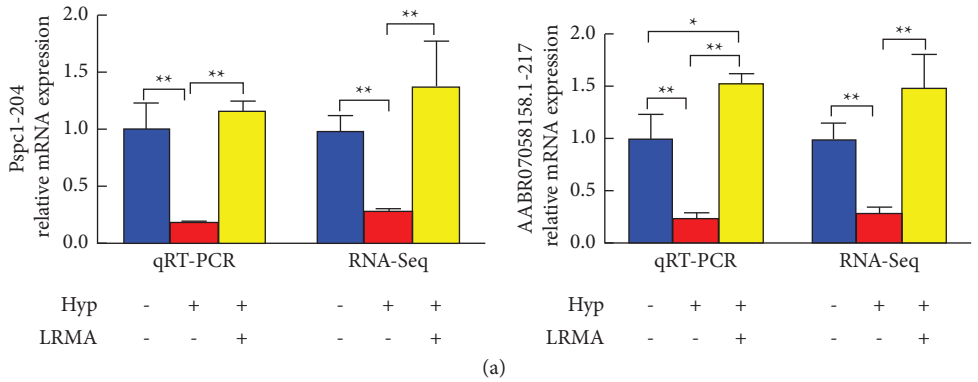

(a)

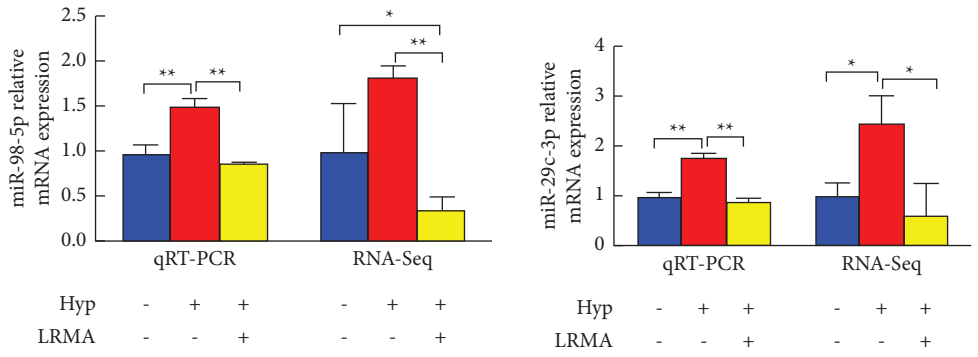

(b)

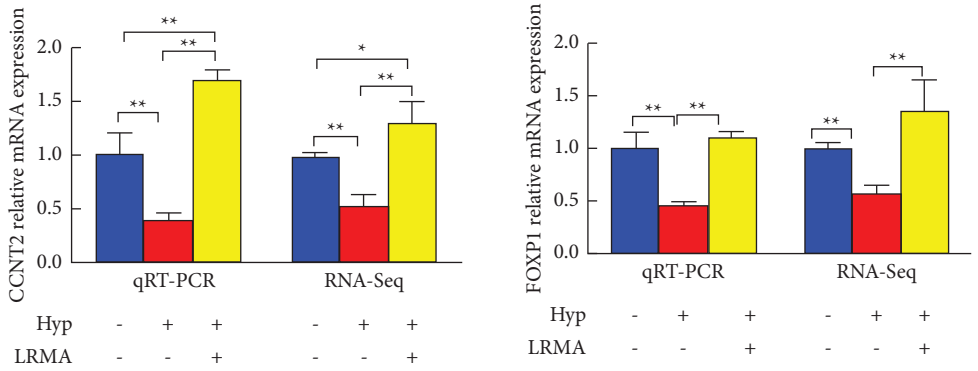

(c)

Figure 4: Continued.

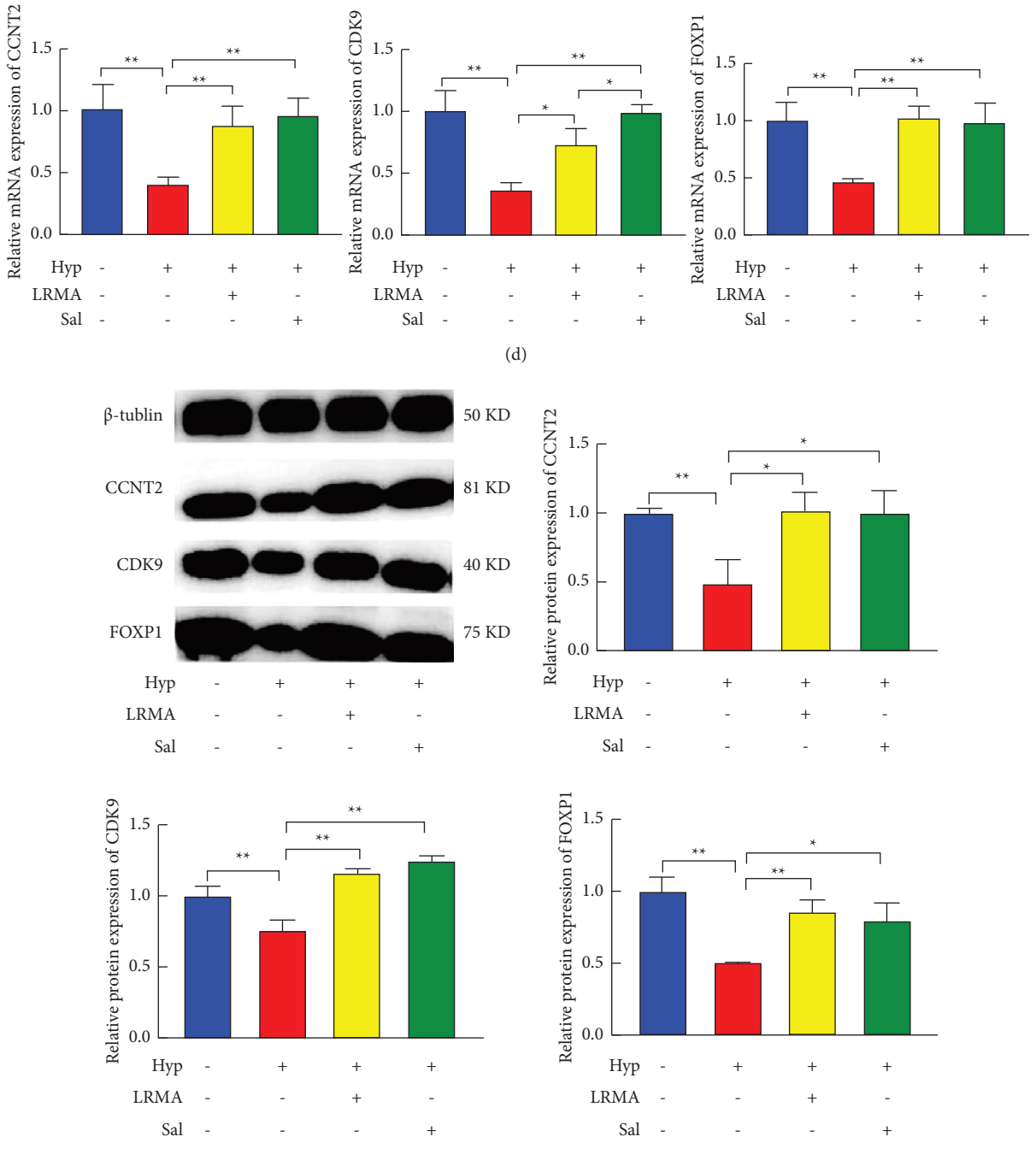

Figure 4: Comparison between qRT-PCR results (left) and RNA-seq results (right). After incubation with 50 μg/mL LRMA for 12 h under normoxia + 24 h under hypoxic condition, lncRNA (a), miRNA (b), and mRNA (c) expressions at RNA level were tested, as well as the effect of LRMA on the proliferation of H9c2 cells under hypoxic condition. After 50 μg/mL LRMA and 100 μM sal incubation for 12 h normoxia + 24 h under the hypoxic condition, respectively, CCNT2, CDK9, and FOXP1 expressions at RNA (d) and protein (e) level were analyzed. $N = 3$. $^{*}P < 0.05$ and $^{**}P < 0.01$. NS: no significance.

Under hypoxic conditions, the LDH content in the cytosol increases, cells undergo morphological changes such as crumpling and deformation, and the cell structure, i.e., the integrity of the cell membrane and normal cell morphology, is damaged. The results of the present experimental study showed that hypoxia caused reduced membrane integrity, destruction of cell morphology and structure, and apoptotic and necrotic morphology in H9c2 rat cardiomyocytes, which is consistent with the results of the previous studies [26, 27]. Apoptosis is a programmed cell death that is complexly

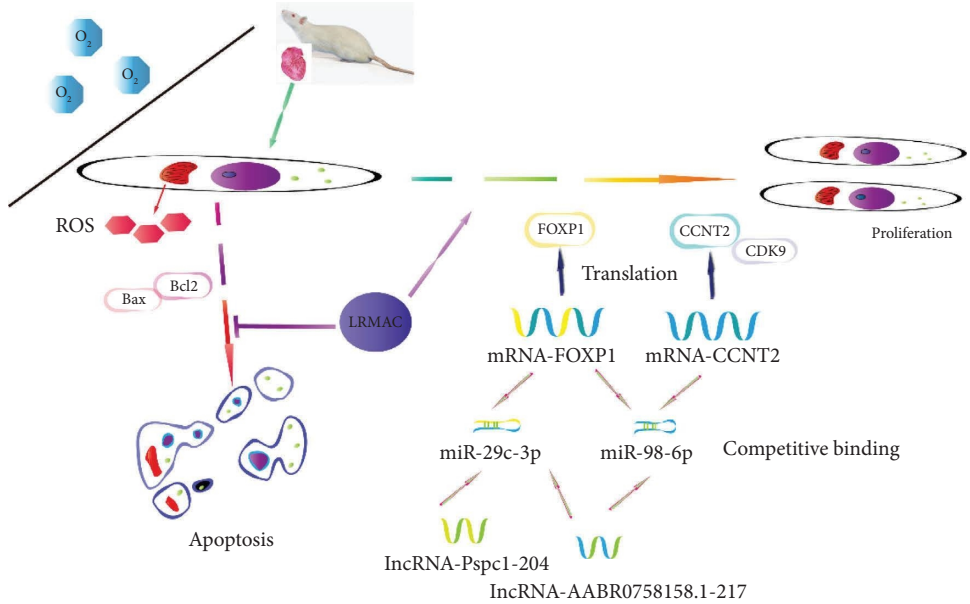

Figure 5: A schematic diagram summarizing the key findings of the study.

regulated by multiple genes and involves activation, expression, and regulation of intracellular-related factors, which have important roles in immune defense and cell damage in animal organisms [28, 29]. The apoptotic process is regulated by several genes, among which the Bcl2 family genes are predominant [30]. Bcl2 and Bax belong to the Bcl2 family with different roles to inhibit and promote apoptosis, respectively. Bcl2 is a representative of apoptosis-inhibiting genes, which can inhibit apoptosis by antagonizing the expression of proapoptotic genes [31]. Bax is a homologue of Bcl2, which binds to Bcl2 to form a heterodimer and then initiates a signaling pathway to promote apoptosis. Bax can antagonize the inhibitory effect of Bcl2 and promote apoptosis, and the ratio of Bax/Bcl2 expression can also reflect apoptosis [32]. Mitochondrial aerobic respiration is the main source of endogenous ROS [33], and hypoxia can lead to the production of large amounts of ROS in cells, which, if not cleared in time, can damage the body's natural antioxidant system and can directly damage cardiomyocytes, protein structures, and DNA and induce apoptosis in cardiomyocytes by upregulating Bcl2 and downregulating Bax expression, thus causing hypoxic body damage and thus affecting the structure and function of the heart [34, 35]. In this experiment, we found that LRMA could effectively inhibit hypoxia-induced ROS content accumulation and apoptosis in H9c2 rat cardiomyocytes and could downregulate the mRNA and protein expression of Bax and upregulate Bcl2 and Bcl2/Bax ratio to inhibit hypoxia-induced apoptosis in H9c2 rat cardiomyocytes under hypoxic conditions, and the inhibitory effect of LRMA on hypoxia-induced apoptosis in H9c2 rat cardiomyocytes under hypoxic conditions was not significantly different from that of Sal.

Most ceRNAs can bind to miRNA by their potential microRNA response elements (MREs) [36]. A number of prior studies have reported that ceRNAs can affect the downstream signal pathway by regulating the number or the function of different miRNAs [37, 38]. The lncRNAs-miRNAs-mRNAs regulatory network, a hot research topic in several fields, can effectively participate in immune regulation, cardiovascular diseases or other important biological processes [39–41]. Besides, various studies have shown that lncRNAs-miRNAs-mRNAs regulatory network can play a protective role in myocardial injury induced by hypoxia. Therefore, we investigated the effect of LRMA on hypoxia-induced mammalian myocardial injury by constructing a hypoxia-related lncRNAs-miRNAs-mRNAs ceRNA network of H9c2 cells regulated by LRMA.

By using RNA-seq technique and biological information analysis, 862 hypoxia-related differentially expressed lncRNAs, 7 miRNAs, and 351 mRNAs were found to be involved in the regulation of LRMA. To predict the function of lncRNAs, this study performed functional enrichment analysis of the source genes involved in the regulation of hypoxia-related differentially expressed lncRNAs in H9c2 rat cardiomyocytes, and the results showed that the hypoxia-related genes regulated by LRMA were mainly enriched in cell proliferation and division, cell energy metabolism, inflammatory response, and cell development. The above functions and pathways may be potential pathways involved in the regulation of LRMA-mediated lncRNAs in hypoxia-induced H9c2 rat cardiomyocytes. Finally, we obtained five different pairs of ceRNAs i.e., ENSRONG09184-ASL-rno-miR-98-6p-FOXP1, AABR0758158.1-217-rno-miR-98-6p-FOXP1, AABR0758158.1-217-rno-miR-29c-3p-FOXP1, AABR0758158.1-217- rno-miR-29c-3p-CCNT2, Pspc1-204-rno-miR-29c-3p-CCNT2, and the qRT-PCR validation results were consistent with the RNA-seq results, indicating that under hypoxic conditions, LRMA significantly regulates the key genes CCNT2 and FOXP1 mRNA expression under hypoxic conditions.

The heterodimer formed by CCNT2/CDK9 has been reported to be functionally distinct from other CDK/cyclin

complexes that can regulate cell cycle processes but maintains structural affinity with these complexes. CCNT2/CDK9 promotes gene transcription extension, cell proliferation, differentiation, and inhibits apoptosis [42]. It was shown that in mouse embryonic stem cells, attenuation of CCNT2/CDK9 inhibits muscle cell proliferation [43]. FOXP1, a member of the P subfamily of the FOX transcription factor superfamily, can effectively promote cardiomyocyte proliferation and myocardial remodeling [44]. In addition, degradation of FOXP1 enhances cellular inflammatory responses and hypoxia-induced injury [45]. In this experiment, we found that LRMA could alleviate the cell cycle arrest of H9c2 rat cardiomyocytes under hypoxic conditions and promote the proliferation of H9c2 rat cardiomyocytes by increasing the mRNA and protein level expression of CCNT2, CDK9, and FOXP1 in hypoxia-induced H9c2 rat cardiomyocytes. And the regulatory effect of LRMA on hypoxia-induced proliferation of H9c2 rat cardiomyocytes under hypoxic conditions was not significantly different from that of Sal. The above results suggest that LRMA may promote hypoxia-induced proliferative effects in H9c2 rat cardiomyocytes through the regulation of lncRNAs-related ceRNA coregulatory network, but the related molecular mechanisms need to be further validated.

5. Conclusions

In this study, the effect of LRMA on the proliferation and apoptosis of H9c2 rat cardiomyocytes under hypoxia was investigated for the first time, and the optimal induction protocol of LRMA under hypoxic conditions was screened: 50 μg/mL LRMA pretreatment for 12 h, and the cells were then placed under hypoxia + LRMA conditions for 24 h. LRMA was able to promote hypoxia-induced proliferation and inhibit apoptosis in H9c2 rat cardiomyocytes, effectively protecting the cellular activity of H9c2 rat cardiomyocytes under hypoxic conditions. This study also found that LRMA may promote the proliferative effect of hypoxia-induced H9c2 rat cardiomyocytes through regulating the coregulatory network of 5 pairs of lncRNAs-related ceRNAs, but the related molecular mechanisms need to be further verified (Figure 5).

Abbreviations

LRMA: *Lycium ruthenicum* Murry anthocyanins
Bax: BCL2-associated X
Bcl2: B-cell lymphoma-2
CCNT2: Cyclin T2
CDK9: Cyclin dependent kinase 9
FOXP1: Forkhead box P1
DMEM: Dulbecco's modified Eagle's medium
FBS: Fetal bovine serum
PBS: Phosphate buffered saline
CCK-8: Cell counting kit-8
LDH: Lactate dehydrogenase
ROS: Reactive oxygen species
BCA: Bicinchoninic acid
SDS-PAGE: Sodium dodecyl-sulfate polyacrylamide gel electrophoresis
PVDF: Polyvinylidene fluoride
Sal: Salidroside
BDNF: Brain-derived neurotrophic factor
p-TEFb: The positive transcription elongation factor b
ceRNA: The competing endogenous RNA
miRNA: MicroRNAs
lncRNA: Long noncoding RNA
MREs: MicroRNA response elements
PI: Propidium lodide.

Data Availability

All relevant data are included within the manuscript and in its supporting information files.

Conflicts of Interest

The authors declare that they have no conflicts of interest.

Authors' Contributions

Hua Wu conceptualized the study, curated the data, supervised the study, and reviewed and edited the article. Jinming Li provided the software, proposed the methodology, wrote the original draft, and reviewed and edited the article. Mengjie Wang performed formal analysis, provided resources, wrote the original draft, and reviewed and edited the article. Xinlei Chen proposed the methodology. Qianwen Xing visualized the study. Tong Shen validated and visualized the study. Shuo Wang investigated the study. Xiaoqing Wu validated the study. All authors have read and agreed to the published version of the manuscript. Jinming Li and Mengjie Wang contributed equally to this work.

Acknowledgments

This research was funded by the National Natural Science Foundation of China (grant number: 32160812) and the Qinghai Provincial Department of Science and Technology (grant number: 2022-ZJ-927).

Supplementary Materials

As mentioned in article 303, hypoxia-related differential expressed lncRNAs, miRNAs, and mRNAs regulated by LRMA have been shown in supplementary materials. Table 1: Differential hypoxia-related lncRNAs regulated by LRMA; Table 2: Differential hypoxia-related miRNAs regulated by LRMA; and Table 3: Differential hypoxia-related mRNAs regulated by LRMA. (*Supplementary Materials*)

References

[1] J. Gao, L. Ke, and Y. Sun, "Progress in the genetic modification of blue flowers based on anthocyanin metabolism," *Chinese Journal of Biotechnology*, vol. 36, no. 4, pp. 678–692, 2020.
[2] J. M. Kong, L. S. Chia, N. K. Goh, T. F. Chia, and R. Brouillard, "Analysis and biological activities of anthocyanins," *Phytochemistry*, vol. 64, no. 5, pp. 923–933, 2003.

[3] Z. Zhang, X. L. Kou, K. Fugal, and J. McLaughlin, "Comparison of HPLC methods for determination of anthocyanins and anthocyanidins in bilberry extracts," *Journal of Agricultural and Food Chemistry*, vol. 52, no. 4, pp. 688–691, 2004.

[4] L. Mazzoni, F. Giampieri, J. M. Alvarez Suarez et al., "Isolation of strawberry anthocyanin-rich fractions and their mechanisms of action against murine breast cancer cell lines," *Food & Function*, vol. 10, no. 11, pp. 7103–7120, 2019.

[5] D. Li, P. Wang, Y. Luo, M. Zhao, and F. Chen, "Health benefits of anthocyanins and molecular mechanisms: update from recent decade," *Critical Reviews in Food Science and Nutrition*, vol. 57, no. 8, pp. 1729–1741, 2017.

[6] J. H. Kwak, Y. Kim, S. I. Ryu et al., "Anti-inflammatory effect from extracts of red Chinese cabbage and aronia in LPS-stimulated RAW 264.7 cells," *Food Science and Nutrition*, vol. 8, no. 4, pp. 1898–1903, 2020.

[7] U. Nöthlings, M. Schulze, C. Weikert et al., "Intake of vegetables, legumes, and fruit, and risk for all-cause, cardiovascular, and cancer mortality in a European diabetic population," *The Journal of Nutrition*, vol. 138, no. 4, pp. 775–781, 2008.

[8] I. Krga and D. Milenkovic, "Anthocyanins: from sources and bioavailability to cardiovascular-health benefits and molecular mechanisms of action," *Journal of Agricultural and Food Chemistry*, vol. 67, no. 7, pp. 1771–1783, 2019.

[9] H. Yu, B. Chen, and Q. Ren, "Baicalin relieves hypoxia-aroused H9c2 cell apoptosis by activating Nrf2/HO-1-mediated HIF1α/BNIP3 pathway," *Artificial Cells, Nanomedicine, and Biotechnology*, vol. 47, no. 1, pp. 3657–3663, 2019.

[10] J. L. Fan, T. T. Zhu, Z. Y. Xue et al., "lncRNA-XIST protects the hypoxia-induced cardiomyocyte injury through regulating the miR-125b-hexokianse 2 Axis," *In Vitro Cellular & Developmental Biology- Animal*, vol. 56, no. 4, pp. 349–357, 2020.

[11] S. Wang, T. Yao, F. Deng et al., "LncRNA MALAT1 promotes oxygen-glucose deprivation and reoxygenation induced cardiomyocytes injury through sponging miR-20b to enhance beclin1-mediated autophagy," *Cardiovascular Drugs and Therapy*, vol. 33, no. 6, pp. 675–686, 2019.

[12] J. Wang, X. Chen, and W. Huang, "MicroRNA-369 attenuates hypoxia-induced cardiomyocyte apoptosis and inflammation via targeting TRPV3," *Brazilian Journal of Medical and Biological Research*, vol. 54, no. 3, Article ID e10550, 2021.

[13] J. Lv, W. Wang, X. Zhu et al., "DW14006 as a direct AMPKα1 activator improves pathology of AD model mice by regulating microglial phagocytosis and neuroinflammation," *Brain, Behavior, and Immunity*, vol. 90, pp. 55–69, 2020.

[14] R. Tian, X. Guan, H. Qian et al., "Restoration of NRF2 attenuates myocardial ischemia reperfusion injury through mediating microRNA-29a-3p/CCNT2 Axis," *BioFactors*, vol. 47, no. 3, pp. 414–426, 2021.

[15] L. Xing, J. Ren, X. Guo, S. Qiao, and T. Tian, "Decitabine shows anti-acute myeloid leukemia potential via regulating the miR-212-5p/CCNT2 Axis," *Open Life Sciences*, vol. 15, no. 1, pp. 1013–1023, 2020.

[16] D. Zhao and Y. Hou, "Long non-coding RNA nuclear-enriched abundant transcript 1 (LncRNA NEAT1) upregulates cyclin T2 (CCNT2) in laryngeal papilloma through sponging miR-577/miR-1224-5p and blocking cell apoptosis," *Bioengineered*, vol. 13, no. 1, pp. 1828–1837, 2022.

[17] Y. Shiozaki, K. Okamura, S. Kohno et al., "The CDK9-cyclin T1 complex mediates saturated fatty acid-induced vascular calcification by inducing expression of the transcription factor CHOP," *Journal of Biological Chemistry*, vol. 293, no. 44, Article ID 17020, 2018.

[18] B. Wang, J. Weidenfeld, M. M. Lu et al., "Foxp1 regulates cardiac outflow tract, endocardial cushion morphogenesis and myocyte proliferation and maturation," *Development*, vol. 131, no. 18, pp. 4477–4487, 2004.

[19] Y. Zhang, S. Li, L. Yuan et al., "Foxp1 coordinates cardiomyocyte proliferation through both cell-autonomous and nonautonomous mechanisms," *Genes & Development*, vol. 24, no. 16, pp. 1746–1757, 2010.

[20] K. L. Adams, D. L. Rousso, J. A. Umbach, and B. G. Novitch, "Foxp1-Mediated programming of limb-innervating motor neurons from mouse and human embryonic stem cells," *Nature Communications*, vol. 6, no. 1, pp. 6778–6794, 2015.

[21] X. W. Tian, *Effect of Wild Baicalin on the Inhibition of Proliferation and Expression of Bcl-2 and Bax in Human Tongue Squamous Carcinoma Tca8113 cells*, Chengde Medical College, Chengde, China, 2013.

[22] J. Chen, "Study on the control and regulatory mechanism of aerobic exercise on the proliferation of rat cardiomyocytes," *Heilongjiang Animal Science and Veterinary Medicine*, vol. 523, no. 7, pp. 246–248, 2017.

[23] J. C. Garbern and R. T. Lee, "Heart regeneration: 20 years of progress and renewed optimism," *Developmental Cell*, vol. 57, no. 4, pp. 424–439, 2022.

[24] X. Y. Wang, M. Li, and Z. G. Shen, "Research progress on the pharmacological effects of Salidroside," *Chinese Traditional Patent Medicine*, vol. 44, no. 12, pp. 3932–3935, 2022.

[25] H. Zhong, H. Xin, L. X. Wu, and Y. Z. Zhu, "Salidroside attenuates apoptosis in ischemi ccardiomyocytes:a mechanism through a mitochondria-dependent pathway," *Journal of Pharmacological Sciences*, vol. 114, no. 4, pp. 399–408, 2010.

[26] Q. T. Huang, Y. M. Xu, and J. Xu, "Hypoxia regulates cell membrane damage after ElMD," *Journal of Shandong Sport University*, vol. 34, no. 4, pp. 81–86, 2018.

[27] S. Wang, Y. Zhang, X. Lin et al., "Learning matrix factorization with scalable distance metric and regularizer," *Neural Networks: The Official Journal of the International Neural Network Society*, vol. 161, no. 2, pp. 254–266, 2023.

[28] M. S. D'Arcy, "Cell death: a review of the major forms of apoptosis, necrosis and autophagy," *Cell Biology International*, vol. 43, no. 6, pp. 582–592, 2019.

[29] G. Pistritto, D. Trisciuoglio, C. Ceci, A. Garufi, and G. D'Orazi, "Apoptosis as anticancer mechanism:function and dysfunction of its modulators and targeted the rapeutic strategies," *Aging*, vol. 8, no. 4, pp. 603–619, 2016.

[30] J. Liang, J. L. Luo, and Q. Q. Cai, "Study on the effect mechanism of iridoid glycosides of scrophularia ningpoensis inhibiting cardiomyocytes apoptosis in myocardial infarction model rats based on different caspase apoptosis pathways," *China Pharmacy*, vol. 30, no. 6, pp. 735–740, 2019.

[31] N. Azarshinfam, A. Tanomand, H. Soltanzadeh, and F. A. Rad, "Evaluation of anticancer effects of propolis extract with or without combination with layered double hydroxide nanoparticles on Bcl-2 and Bax genes expression in HT-29 cell-lines," *Gene Reports*, vol. 23, Article ID 101031, 2021.

[32] G. T. Shao, X. L. Chen, and L. F. Shao, "Mechanism of p38 signaling pathway on proliferation and apoptosis of astrocytes under hypoxia," *Journal of Clinical and Experimental Medicine*, vol. 16, no. 13, pp. 1252–1255, 2017.

[33] P. Willems, R. Rossignol, C. Dieteren, M. Murphy, and W. Koopman, "Redox homeostasis and mitochondrial dynamics," *Cell Metabolism*, vol. 22, no. 2, pp. 207–218, 2015.

[34] J. Yang and F. Gao, "Advances in the study of reactive oxygen species and apoptosis[J]," *Journal of International Oncology*, vol. 4, pp. 248–251, 2002.

[35] X. Cao, M. Fu, R. Bi et al., "Cadmium induced BEAS-2B cells apoptosis and mitochondria damage via MAPK signaling pathway," *Chemosphere*, vol. 263, no. 6, Article ID 128346, 2021.

[36] X. Xu, Y. Lai, and Z. C. Hua, "Apoptosis and apoptotic body: disease message and therapeutic target potentials," *Bioscience Reports*, vol. 39, no. 1, Article ID 20180992, 2019.

[37] S. Qu, X. Yang, X. Li et al., "Circular RNA: a new star of noncoding RNAs," *Cancer Letters*, vol. 365, no. 2, pp. 141–148, 2015.

[38] C. Wang, H. Zi, Y. Wang, B. Li, Z. Ge, and X. Ren, "Retracted article: LncRNA *CASC15* promotes tumour progression through *SOX4*/Wnt/*β*-catenin signalling pathway in hepatocellular carcinoma," *Artificial Cells, Nanomedicine, and Biotechnology*, vol. 48, no. 1, pp. 763–769, 2020.

[39] Z. Yuan and W. Wang, "LncRNA SNHG4 regulates miR-10a/PTEN to inhibit the proliferation of acute myeloid leukemia cells," *Hematology*, vol. 25, no. 1, pp. 160–164, 2020.

[40] R. Masvekar, T. Wu, P. Kosa, C. Barbour, V. Fossati, and B. Bielekova, "Cerebrospinal fluid biomarkers link toxic astrogliosis and microglial activation to multiple sclerosis severity," *Multiple Sclerosis and Related Disorders*, vol. 28, pp. 34–43, 2019.

[41] K. Zheng, F. Hu, Y. Zhou et al., "miR-135a-5p mediates memory and synaptic impairments via the rock2/adducin1 signaling pathway in A mouse model of alzheimer's disease," *Nature Communications*, vol. 12, no. 1, pp. 1903–1919, 2021.

[42] Y. Cai, X. Li, Z. Pan et al., "Anthocyanin ameliorates hypoxia and ischemia induced inflammation and apoptosis by increasing autophagic flux in SH-SY5Y cells," *European Journal of Pharmacology*, vol. 883, Article ID 173360, 2020.

[43] C. Simone, L. Bagella, C. Bellan, and A. Giordano, "Physical Interaction between pRb and cdk9/cyclinT2 Complex," *Oncogene*, vol. 21, no. 26, pp. 4158–4165, 2002.

[44] J. Kohoutek, Q. Li, D. Blazek, Z. Luo, H. Jiang, and B. M. Peterlin, "Cyclin T2 is essential for mouse embryogenesis," *Molecular and Cellular Biology*, vol. 29, no. 12, pp. 3280–3285, 2009.

[45] M. De Falco and A. De Luca, "Involvement of cdks and cyclins in muscle differentiation," *European Journal of Histochemistry: EJH*, vol. 50, no. 1, pp. 19–23, 2006.